

Fast Particle Tracking With Wake Fields

M. Dohlus, K. Flöttmann, C. Henning

Abstract

Tracking calculations of charged particles in electromagnetic fields require in principle the simultaneous solution of the equation of motion and of Maxwell's equations. In many tracking codes a simpler and more efficient approach is used: external fields like that of the accelerating structures are provided as field maps, generated in separate computations and for the calculation of self fields the model of a particle bunch in uniform motion is used. We describe how an externally computed wake function can be approximated by a table of Taylor coefficients and how the wake field kick can be calculated for the particle distribution in a tracking calculation. The integrated kick, representing the effect of a distributed structure, is applied at a discrete time. As an example, we use our approach to calculate the emittance growth of a bunch in an undulator beam pipe due to resistive wall wake field effects.

INTRODUCTION

Self consistent particle tracking needs the simultaneous solution of the equation of motion for a multi particle system ($N \sim 10^3 \dots 10^9$) and of Maxwell's equations. The effort is usually rather high, as the electro-magnetic field calculation in time domain has to resolve the dimension of the bunch and of the surrounding geometry: a large volume has to be discretized with high resolution, and a good spatial resolution is related to a fine time step [1].

Supposed the particle energy is high enough for ultra-relativistic approximations, the motion is approximately uniform and the betatron wavelength is large compared to geometric dimensions as cavities, magnets and wake generating discontinuities. Then the electromagnetic problem can be split into independent sub-problems: external fields, wake field interactions and simplified self-interactions. The separation of external fields is possible without these conditions, but the wake field approach is based on an idealised setup as sketched in Fig. 1: a discontinuity, either of geometry or of material properties or of both, is enclosed by semi-infinite beam pipes. Several generations of wake field codes have been developed to solve this problem [2–6]. The model of simplified self interactions calculates so called “space charge forces” for a particle distribution in uniform motion, using a Lorentz transformation and solving an electrostatic field [8–10].

This report is about the application of wake fields in a tracking program. The effect of a distributed wakefield generating structure is replaced by a discrete kick at a discrete time, calculated from a wake function that is determined with help of a wake field code. The wake function has to be described by a flexible format. We propose a hybrid formulation: the dependency on the longitudinal coordinate s (between source and observer particle) is tabulated and the transverse dependency (offset of source and observer particle) is Taylor expanded. Therefore the wake function is stored in a table of Taylor coefficients. The point to point interaction between all particles is calculated by a convolution method. Therefore the line charge density and generalized line charge densities (the first and second transverse moments) are calculated on a grid by a binning and smoothing technique.

Our method is implemented in the space charge code ASTRA [9]. As an example we calculate the emittance growth of a bunch in an undulator beam pipe due to resistive wall wake field effects. In this example the wake per length in a 30 m beam pipe is modeled

by about 60 diskrete kicks. The example considers a real focussing lattice, collective and individual transverse motion and simultaneously longitudinal and transverse effects (which cannot be separated from each other).

COORDINATE SYSTEM AND WAKE FUNCTION

The particles are tracked in global Cartesian coordinates with (x, y, z, p_x, p_y, p_z) , the components of location and momentum, while wake fields are calculation in a local coordinate system with (u, v, w, p_u, p_v, p_w) components. The coordinates of both systems are related by:

$$\begin{pmatrix} \vec{e}_x & \vec{e}_y & \vec{e}_z \end{pmatrix} \begin{pmatrix} x_n \\ y_n \\ z_n \end{pmatrix} = \vec{r}_o + \begin{pmatrix} \vec{e}_u & \vec{e}_v & \vec{e}_w \end{pmatrix} \begin{pmatrix} u_n \\ v_n \\ w_n \end{pmatrix} \quad (1)$$

$$\begin{pmatrix} \vec{e}_x & \vec{e}_y & \vec{e}_z \end{pmatrix} \begin{pmatrix} p_{x,n} \\ p_{y,n} \\ p_{z,n} \end{pmatrix} = \begin{pmatrix} \vec{e}_u & \vec{e}_v & \vec{e}_w \end{pmatrix} \begin{pmatrix} p_{u,n} \\ p_{v,n} \\ p_{w,n} \end{pmatrix} \quad (2)$$

with n the particle index, \vec{r}_o the vector to the origin of the wake geometry, \vec{e}_w the unity vector into nominal direction of particle motion and \vec{e}_u, \vec{e}_v the orthonormal transverse vectors. The discrete wake induced kicks are added to the particle momenta when the center of mass of the distribution passes the plane $\vec{r}_o + u\vec{e}_u + v\vec{e}_v$. The setup is sketched in Fig. 1.

For simplicity we set $\vec{r}_o = \vec{0}$ for the following. A source particle with charge q_s on the trajectory $\vec{r}_s(t) = u_s\vec{e}_u + v_s\vec{e}_v + ct\vec{e}_w$ is followed by a observer particle with charge q_o and trajectory $\vec{r}_o(t) = u_o\vec{e}_u + v_o\vec{e}_v + (ct - s)\vec{e}_w$. The source particle causes the electromagnetic field $\vec{E}^{(s)}, \vec{B}^{(s)}$. The total change of momentum of the observer particle is

$$\Delta\vec{p} = q_o \int_{-\infty}^{\infty} \left(\vec{E}^{(s)}(\vec{r}_o(t), t) + c\vec{e}_w \times \vec{B}^{(s)}(\vec{r}_o(t), t) \right) dt. \quad (3)$$

For the definition of the wake function we follow [7] with

$$\vec{w}_f(u_s, v_s, u_o, v_o, s) = \frac{c}{q_o q_s} \Delta\vec{p}. \quad (4)$$

The wake function is causal in the s coordinate, the transverse and longitudinal components

are related by the Panofsky-Wenzel-Theorem

$$\frac{\partial}{\partial s}(\vec{w}_f \cdot \vec{e}_u) = -\frac{\partial}{\partial u_o}(\vec{w}_f \cdot \vec{e}_w) , \quad (5)$$

$$\frac{\partial}{\partial s}(\vec{w}_f \cdot \vec{e}_v) = -\frac{\partial}{\partial v_o}(\vec{w}_f \cdot \vec{e}_w) , \quad (6)$$

and the longitudinal component is a harmonic function of transverse coordinates

$$\left(\frac{\partial^2}{\partial u_o^2} + \frac{\partial^2}{\partial v_o^2} \right) (\vec{w}_f \cdot \vec{e}_w) = 0. \quad (7)$$

For the following we use scalar component functions

$$\vec{w}_f(u_s, v_s, u_o, v_o, s) = - \begin{pmatrix} \vec{e}_u & \vec{e}_v & \vec{e}_w \end{pmatrix} \begin{pmatrix} h_u(u_s, v_s, u_o, v_o, s) \\ h_v(u_s, v_s, u_o, v_o, s) \\ h_w(u_s, v_s, u_o, v_o, s) \end{pmatrix}. \quad (8)$$

The implementation of wake fields in Astra is based on a second order Taylor expansion of the longitudinal wake in the transverse coordinates

$$h_w(u_s, v_s, u_o, v_o, s) = \begin{bmatrix} 1 \\ u_s \\ v_s \\ u_o \\ v_o \end{bmatrix}^t \begin{bmatrix} h_{00}(s) & h_{01}(s) & h_{02}(s) & h_{03}(s) & h_{04}(s) \\ 0 & h_{11}(s) & h_{12}(s) & h_{13}(s) & h_{14}(s) \\ 0 & h_{12}(s) & h_{22}(s) & h_{23}(s) & h_{24}(s) \\ 0 & h_{13}(s) & h_{23}(s) & h_{33}(s) & h_{34}(s) \\ 0 & h_{14}(s) & h_{24}(s) & h_{34}(s) & -h_{33}(s) \end{bmatrix} \begin{bmatrix} 1 \\ u_s \\ v_s \\ u_o \\ v_o \end{bmatrix}. \quad (9)$$

This approach fulfills Eq. (7). The transverse components are uniquely related to the longitudinale wake by causality and Panofsky-Wenzel-Theorem:

$$h_u(u_s, v_s, u_o, v_o, s) = h_{03}^{(i)}(s) + 2h_{13}^{(i)}(s)u_s + 2h_{23}^{(i)}(s)v_s + 2h_{33}^{(i)}(s)u_o + 2h_{34}^{(i)}(s)v_o , \quad (10)$$

$$h_v(u_s, v_s, u_o, v_o, s) = h_{04}^{(i)}(s) + 2h_{14}^{(i)}(s)u_s + 2h_{24}^{(i)}(s)v_s + 2h_{34}^{(i)}(s)u_o - 2h_{33}^{(i)}(s)v_o , \quad (11)$$

with the integrated coefficient functions

$$h_{\alpha\beta}^{(i)}(s) = - \int_{-\infty}^s h_{\alpha\beta}(x) dx . \quad (12)$$

Special cases for geometries with symmetry of revolution are the monopole and dipole wake.

The monopole wake

$$\vec{w}_f(u_s, v_s, u_o, v_o, s) = -h_{00}(s)\vec{e}_w \quad (13)$$

is purely longitudinal and independent on offset parameters. The transverse part of the dipole wake depends linear on the offset of the source particle. Due to symmetry the coefficient functions $h_{13}(s)$ and $h_{24}(s)$ are identical. Therefore the dipole wake functions is

$$\vec{w}_f(u_s, v_s, u_o, v_o, s) = -(u_s \vec{e}_u + v_s \vec{e}_v) 2h_{13}^{(i)}(s) - (u_s u_o + v_s v_o) \vec{e}_w 2h_{13}(s) . \quad (14)$$

DISTRIBUTED SOURCE

For an arbitrary distribution of source particles with charges $q_{s,n}$, total charge $q_b = \sum q_{s,n}$ and trajectories $\vec{r}_{s,n}(t) = u_{s,n} \vec{e}_u + v_{s,n} \vec{e}_v + (ct + w_{s,n}) \vec{e}_w$, the change of momentum of the observer particle is

$$\Delta \vec{p} = \frac{q_o}{c} \sum_n q_{s,n} \vec{w}_f(u_{s,n}, v_{s,n}, u_o, v_o, s - w_{s,n}) . \quad (15)$$

The wake potential

$$\vec{W}(u_o, v_o, s) = \frac{1}{q_b} \sum_n q_{s,n} \vec{w}_f(u_{s,n}, v_{s,n}, u_o, v_o, s - w_{s,n}) . \quad (16)$$

characterises the shape dependent wake kick. It can be computed with electromagnetic field calculation programs as [2, 3, 6] for continuous gaussian source distributions. Usually the wake function is extrapolated from wake potential computations for small source distributions.

The particle summation in Eq. (15) is replaced by a volume integration

$$\Delta \vec{p} = \frac{q_o}{c} \int \varrho(\tilde{u}, \tilde{v}, \tilde{w}) \vec{w}_f(\tilde{u}, \tilde{v}, u_o, v_o, s - \tilde{w}) d\tilde{u} d\tilde{v} d\tilde{w} \quad (17)$$

with $\varrho(u, v, w)$ the charge density. Formally this can be expressed with a Taylor expansion of the wake function as

$$\Delta \vec{p} = \frac{q_o}{c} \int \varrho(\tilde{u}, \tilde{v}, \tilde{w}) \sum_{ijmn} (\vec{w}_{ijmn}(s - \tilde{w}) \tilde{u}^i \tilde{v}^j u_o^m v_o^n) d\tilde{u} d\tilde{v} d\tilde{w} . \quad (18)$$

Changing the order of summation and integration $\Delta \vec{p}$ can be written as sum of one dimensional convolution integrals

$$\Delta \vec{p} = \frac{q_o}{c} \sum_{ijmn} u_o^m v_o^n \int \lambda_{ij}(\tilde{w}) \vec{w}_{ijmn}(s - \tilde{w}) d\tilde{w} , \quad (19)$$

with scalar functions

$$\lambda_{ij}(\tilde{w}) = \int \varrho(\tilde{u}, \tilde{v}, \tilde{w}) \tilde{u}^i \tilde{v}^j d\tilde{u} d\tilde{v} , \quad (20)$$

and $\vec{w}_{ijmn}(s)$ described in Tab. I. $\lambda_{00}(w)$ is the line charge density. In the following we call $\lambda_{ij}(w)$ generalized line charge densities.

NUMERICAL REALIZATION

For the numerical kick calculations three problems have to be solved: the calculation of generalized one dimensional density functions $\lambda_{ij}(s)$, the representation of coefficient functions $h_{\alpha\beta}(s)$ and the convolution of these functions.

Binning and Smoothing

A *continuization* based on a binning and smoothing technique is used to convert the particle set with longitudinal positions $\{w_n\}$ and discrete generalized charges $\{q_{s,n} u_n^i v_n^j\}$ to continuous generalized line charge densities $\lambda_{ij}(s)$. Conventional binning distributes the particle charges to N_{bin} equi-spaced bins ranging over the whole bunch length. The disadvantages are a spacial resolution independent on particle density, and the bin boundaries are determined by extreme particles (first and last particle). To achieve more flexibility, we use bins that fulfill requirements for the length per bin as well as for the charge per bin, and we utilize a multiple binning with N_{sub} different conditions for the first and last bin.

Therefore the bunch is split into $N_{bin} N_{sub}$ sub-bins. All inner bins are composed by N_{sub} consecutive sub-bins, the outer bins may combine less sub-bins, as sketched in Fig. 2. By doing this, N_{sub} different binnings are generated.

The sub-binning is controlled by the linear combination $f(w) = W_{eq} f_w(w) + (1 - W_{eq}) f_q(w)$ of two auxiliary functions $f_w(w)$ and $f_q(w)$. These functions increase along the bunch monotonously from zero to one. Function $f_w(w)$ is proportional to length while $f_q(w)$ increases with the integrated bunch charge. The boundaries b_k of the sub-bins are the solutions of $f(b_k) = k / (N_{bin} N_{sub})$. Setting W_{eq} to one causes equi-spaced sub-bins, zero leads to equi-charged sub-bins and a middle value generates a mixture of both conditions. The same bins and sub-bins are used for all generalized charges.

Result of the binning procedure are $N_{bin} N_{sub} + N_{sub} - 1$ different bins, each characterized

by the bin center $b_{c,k} = (b_k + b_{k+N_{sub}})/2$, the bin width $b_{w,k} = (b_{k+N_{sub}} - b_k)$ and the bin weights (the sums of generalized charges)

$$Q_{ij,k} = \frac{1}{N_{sub}} \sum_{n \in \text{bin}_k} q_{s,n} u_n^i v_n^j .$$

The smoothing procedure replaces all bins by continuous functions with certain centers, widths and weights and samples the sum of these functions on an equidistant grid:

$$\lambda_{ij,n} = \lambda_{ij}(n\Delta w) , \quad (21)$$

$$\lambda_{ij}(w) = \sum_k \frac{Q_{ij,k}}{b_{w,k}} S\left(\frac{w - b_{c,k}}{b_{w,k}}\right) . \quad (22)$$

The ASTRA implementation uses rectangular, triangular and gaussian smoothing functions:

$$\begin{aligned} S_r(x) &= \begin{cases} 1 & |x| < 0.5 \\ 0 & \text{otherwise} \end{cases} , \\ S_t(x) &= \max(0, 1 - |x|) , \\ S_g(x) &= \frac{1}{\sqrt{2\pi}p} \exp\left(-\frac{x^2}{2p^2}\right) , \end{aligned}$$

with $p \sim 1$, a control parameter. The grid density is determined by the smallest bin width.

Representation of Coefficient Functions

Each coefficient function $h_{\alpha\beta}(s)$ is described by coefficients $R_{\alpha\beta}, L_{\alpha\beta}, \tilde{C}_{\alpha\beta}$ and limited auxiliary functions $q_{\alpha\beta}(s), p_{\alpha\beta}(s)$. For the following we skip the index. The representation is

$$h(s) = q(s) + \frac{\Phi(s)}{C} + Rc\delta(s) - c\frac{\partial}{\partial s} [Lc\delta(s) + p(s)] , \quad (23)$$

with $\delta(s)$ the dirac function, $\Phi(s)$ the step function and $C = \tilde{C}$ if $\tilde{C} \neq 0$. The term with $1/C$ is skipped for $\tilde{C} = 0$. The representation is not unique, but very flexible: every coefficient R, L, C might vanish and the auxiliary functions might be identical to zero. The auxiliary functions are polygons as sketched in Fig. 3. The table description of auxiliary function $h_{\alpha\beta}(s)$ is listed in Tab. II. The entry " $10\alpha + \beta$ " describes the subscript of the auxiliary function. For a complete wake field representation all sub-tables of non vanishing coefficient functions are stacked to one table

$$\text{Table} = \text{stack} \left(\left[\begin{array}{cc} N_t & 0 \end{array} \right], \text{Table1}, \text{Table2} \dots \right) ,$$

with N_t the number of sub-tables. The order of sub-tables is arbitrary, vanishing coefficients need no representation.

Convolution

According to Eqs. (19,20) we need convolution integrals of generalized charges with coefficient functions and integrated coefficient functions:

$$\begin{aligned} H(s) &= \int \lambda(x) h(s-x) dx , \\ H^{(i)}(s) &= \int \lambda(x) h^{(i)}(s-x) dx . \end{aligned}$$

For simplicity we skipped all lower indices. Using the representation Eq. (23) and auxiliary functions

$$\begin{aligned} A(s) &= q(s) + \Phi(s)/C , \\ B(s) &= -cp(s) , \\ Q(s) &= \int_{-\infty}^s q(\tilde{s}) d\tilde{s} , \\ C(s) &= -Q(s) + cp(s) - (s/C + Rc)\Phi(s) , \end{aligned}$$

the convolutions can be rewritten as

$$H(s) = Rc\lambda(x) - Lc^2\lambda'(x) + \int \lambda(x) A(s-x) dx + \int \lambda'(x) B(s-x) dx , \quad (24)$$

$$H^{(i)}(s) = Lc^2\lambda(x) + \int \lambda(x) C(s-x) dx . \quad (25)$$

The integrals are solved piecewise for the generalized charged densities Eq. (22) and polygonal coefficient functions.

EXAMPLE

The example of particle motion in an undulator vacuum chamber with resistive wall wake fields is based on parameters used in [11], see Tab. III. For the calculation with ASTRA, a round stainless steel beam pipe with radius $r_b = 4.75$ mm is used to cause significant transverse effects. The undulator chamber of the real facility (FLASH) is made from aluminium. For the numerical simulation 63 quadrupoles of the FODO lattice are considered and the

resistive wall wake of the 30 m beam pipe is simulated by 62 discrete wake kicks (each for $\Delta L = L_{FODO}/2$) applied in the middle of the drifts between the quadrupoles.

The longitudinal wake per length of a round resistive beam pipe is approximated by

$$\vec{w}_f(u_s, v_s, u_o, v_o, s) \cdot \vec{e}_w = w_r(s) \left(1 + 2 \frac{u_s u_o + v_s v_o}{r_b^2} \right) , \quad (26)$$

with

$$\begin{aligned} w_r(s) &= -\frac{1}{2\pi} \int Z_r(\omega) \exp(j\omega s/c) d\omega , \\ Z_r(\omega) &= \frac{Z_s(\omega)}{2\pi r_b} (1 + j\omega \varepsilon Z_s(\omega) r_b/2)^{-1} , \\ Z_s(\omega) &= \sqrt{j\omega \mu / \kappa(\omega)} , \end{aligned}$$

μ the permeability, ε the permittivity of vacuum and $\kappa(\omega)$ the frequency dependent conductivity of the pipe [11, 12]. therefore only three coefficient functions

$$\begin{aligned} h_{00}(s) &= -\Delta L w_r(s) , \\ h_{13}(s) &= -\frac{\Delta L w_r(s)}{r_b^2} , \\ h_{24}(s) &= -\frac{\Delta L w_r(s)}{r_b^2} , \end{aligned}$$

have to be calculated that are all proportional to $w_r(s)$, the longitudinal resistive wall wake per length. In the wake table the coefficients N_p , R , L und \tilde{C} are set to zero (for $\alpha\beta = 00$, 13 and 24), only the auxiliary functions $u_{00}(s)$, $u_{13}(s)$ and $u_{24}(s)$ are used. In Figs. 4 the emittance growth due to dipole wake forces is shown along the undulator and compared with the analytic estimation from [11]. The numerical result agrees well with the estimation, but the dipole model is incomplete. Fig. 5 shows the emittance growth due to monopole and dipole wake fields. The longitudinal wake causes an energy spread of about 2.4 MeV after 30 meters. For off axis particles with that energy spread, the quadrupole focussing is significantly altered and the transverse emittance is further increased.

ACKNOWLEDGEMENTS

We thank Torsten Limberg, Rainer Wanzenberg and Igor Zagorodnov for useful discussions and comments on this work.

-
- [1] S. Schnepf, E. Gjonaj, T. Weiland: On the Development of a Self-Consistent Particle-In-Cell (PIC) Code Using a Time-Adaptive Mesh Technique. Proceedings of the 10th European Particle Accelerator Conference (EPAC 2006) (EPAC 2006), June 01.07.2006, pp. 2182-2184
 - [2] T. Weiland: Comment on Wakefield Computation in the Time Domain (TBCI). NIM-A 216, pp. 31-34, 1983.
 - [3] MAFIA Collaboration, MAFIA manual, CST GmbH, Darmstadt, 1997.
 - [4] I. Zagorodnov: Indirect methods for wake potential integration. Phys. Rev. ST Accel. Beams 9, 2006.
 - [5] H. Henke and W. Bruns, in Proceedings of EPAC 2006, Edinburgh, Scotland (WEPOCH10, 2006).
 - [6] E. Gjonaj, T. Lau, T. Weiland: Computation of Short Range Wake Fields with PBCI. ICFA Beam Dynamics Newsletter (ICFA 2008), April 01.04.2008, pp. 38-52
 - [7] T. Weiland, R. Wanzenberg: Wake Fields and Impedances, DESY M-91-06.
 - [8] L.M. Young: "PARMELA" Los Alamos National Laboratory report LA-UR-96-1835 (Revised April 22, 2003).
 - [9] K. Flöttman, "ASTRA", DESY, Hamburg, www.desy.de/~mpyf10, 2000.
 - [10] S. van der Geer, O. Luiten, M. de Loos, G. Pöplau, U. van Rienen: 3D space-charge model for GPT simulations of high brightness electron bunches, Institute of Physics Conference Series, No. 175, (2005), p. 101.
 - [11] H. Schlarb, Resistive Wall Wake Fields, Diploma Thesis 1997.
 - [12] K. Bane: The Short-Range Resistive Wall Wakefields. SLAC-PUB-95-7074, Dec. 1995.

i	j	m	n	$\vec{w}_{ijmn}(s) \cdot \vec{e}_u$	$\vec{w}_{ijmn}(s) \cdot \vec{e}_v$	$\vec{w}_{ijmn}(s) \cdot \vec{e}_w$
0	0	0	0	$-h_{03}^{(i)}(s)$	$-h_{04}^{(i)}(s)$	$-h_{00}(s)$
1	0	0	0	$-2h_{13}^{(i)}(s)$	$-2h_{14}^{(i)}(s)$	$-h_{01}(s)$
0	1	0	0	$-2h_{23}^{(i)}(s)$	$-2h_{24}^{(i)}(s)$	$-h_{02}(s)$
0	0	1	0	$-2h_{33}^{(i)}(s)$	$-2h_{34}^{(i)}(s)$	$-h_{03}(s)$
0	0	0	1	$-2h_{34}^{(i)}(s)$	$-2h_{44}^{(i)}(s)$	$-h_{04}(s)$
2	0	0	0	0	0	$-h_{11}(s)$
1	1	0	0	0	0	$-2h_{12}(s)$
1	0	1	0	0	0	$-2h_{13}(s)$
1	0	0	1	0	0	$-2h_{14}(s)$
0	2	0	0	0	0	$-h_{22}(s)$
0	1	1	0	0	0	$-2h_{23}(s)$
0	1	0	1	0	0	$-2h_{24}(s)$
0	0	2	0	0	0	$-h_{33}(s)$
0	0	1	1	0	0	$-2h_{34}(s)$
0	0	0	2	0	0	$h_{33}(s)$

TABLE I: $\vec{w}_{ijmn}(s)$ function.

N_q	N_p
$R \quad /(\text{Us})$	$L \quad /(\text{Us}^2)$
$\tilde{C} \quad /(\text{1/U})$	$10\alpha + \beta$
$s_{q,1} \quad /m$	$q(s_{q,1}) \quad /U$
$s_{q,2} \quad /m$	$q(s_{q,2}) \quad /U$
...	...
$s_{q,N_q} \quad /m$	$q(s_{q,N_q}) \quad /U$
$s_{p,1} \quad /m$	$p(s_{p,1}) \quad /(\text{Us})$
$s_{p,2} \quad /m$	$p(s_{p,2}) \quad /(\text{Us})$
...	... $/(\text{Us})$
$s_{p,N_q} \quad /m$	$p(s_{p,N_p}) \quad /(\text{Us})$

TABLE II: Sub-table of auxiliary function $h_{\alpha\beta}(s)$. The unit U is V/As for $\alpha\beta = 00$, V/(Asm) for $\alpha\beta = 01 \cdots 04$ and V/(Asm²) for all other coefficients.

variable		units	values
beam energy	E_0	GeV	1
bunch charge	Q_0	nC	1
rms bunch length	σ_z	μm	50.0
normalized emittance in the undulator	ϵ^n	μm	2.0
undulator length	L	m	30.0
undulator gap	g	mm	12.0
pipe thickness (minimum)	t	mm	1.25
beam optics beta function	$\bar{\beta}$	m	3
FODO period length	L_{FODO}	m	0.96
Length of FODO quad	L_{FODO}	mm	136.5

TABLE III: Parameters for wake field calculation in undulator as assumed for TTF2.

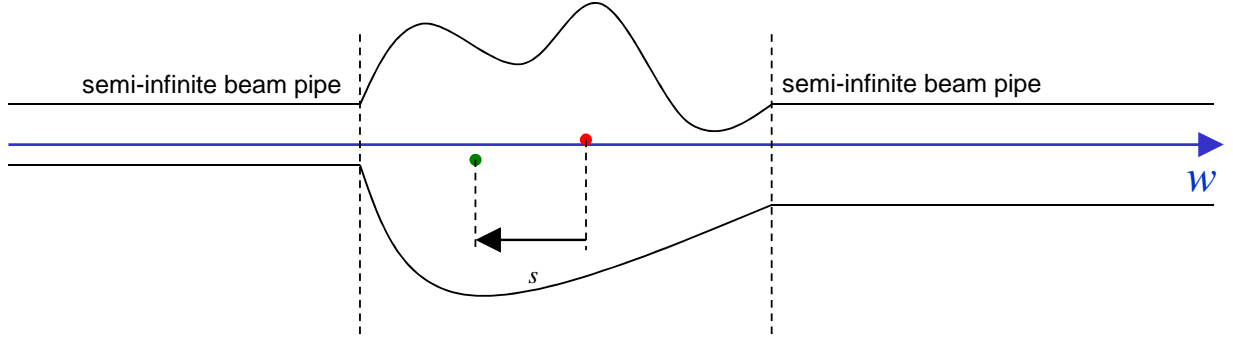


FIG. 1: Source particle (red) and observer particle (green) in a cavity between semi infinite beam pipes.

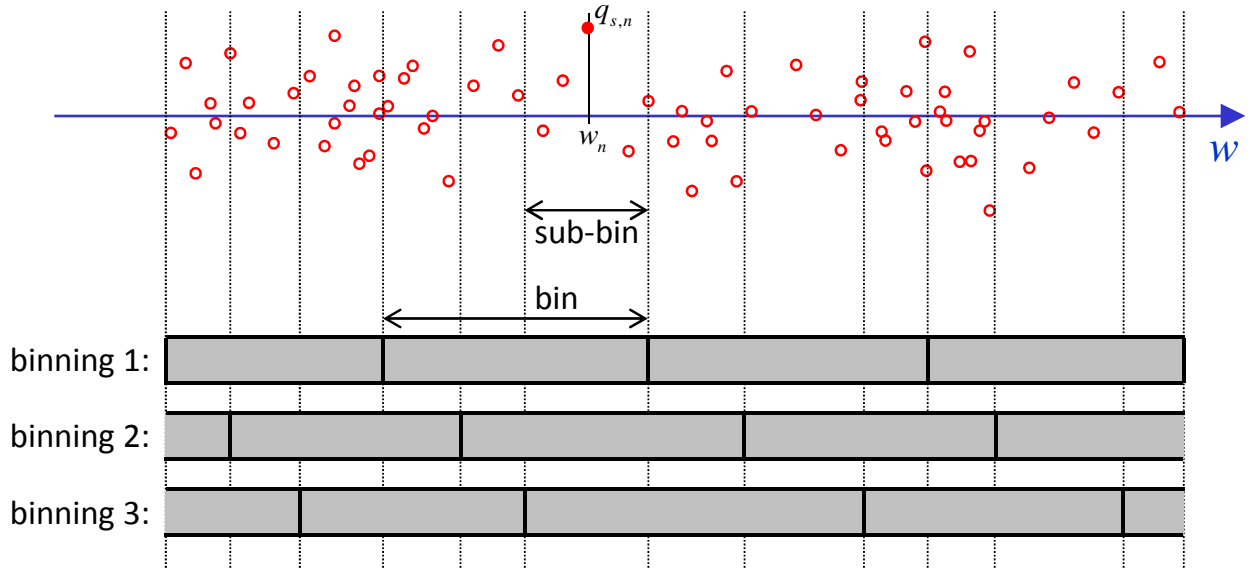


FIG. 2: Binning and sub-binning for $N_{bin} = 4$ and $N_{sub} = 3$.

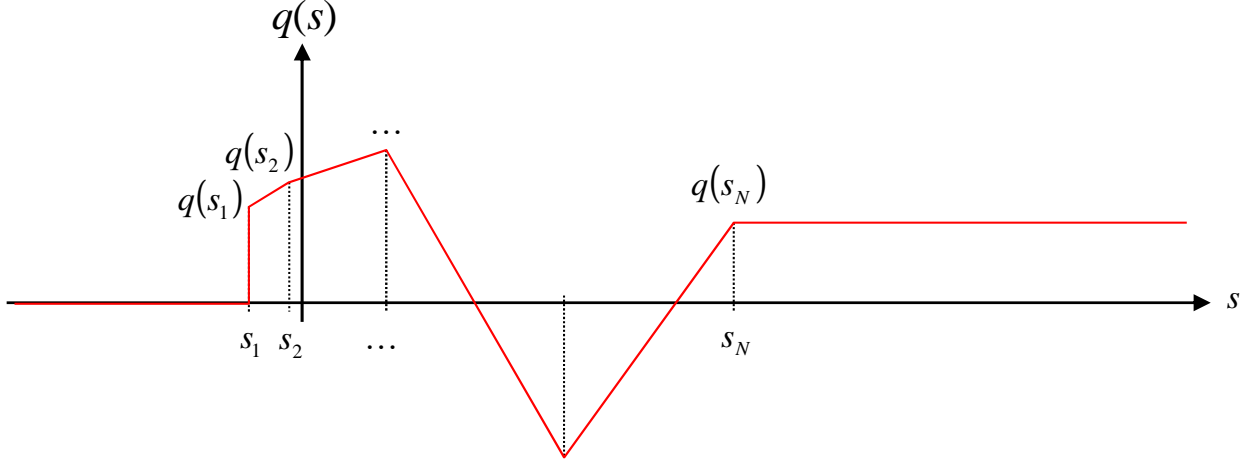


FIG. 3: Auxiliary function $q(s)$ of polygonal shape, with $s_1 < s_2 < \dots < s_N$.

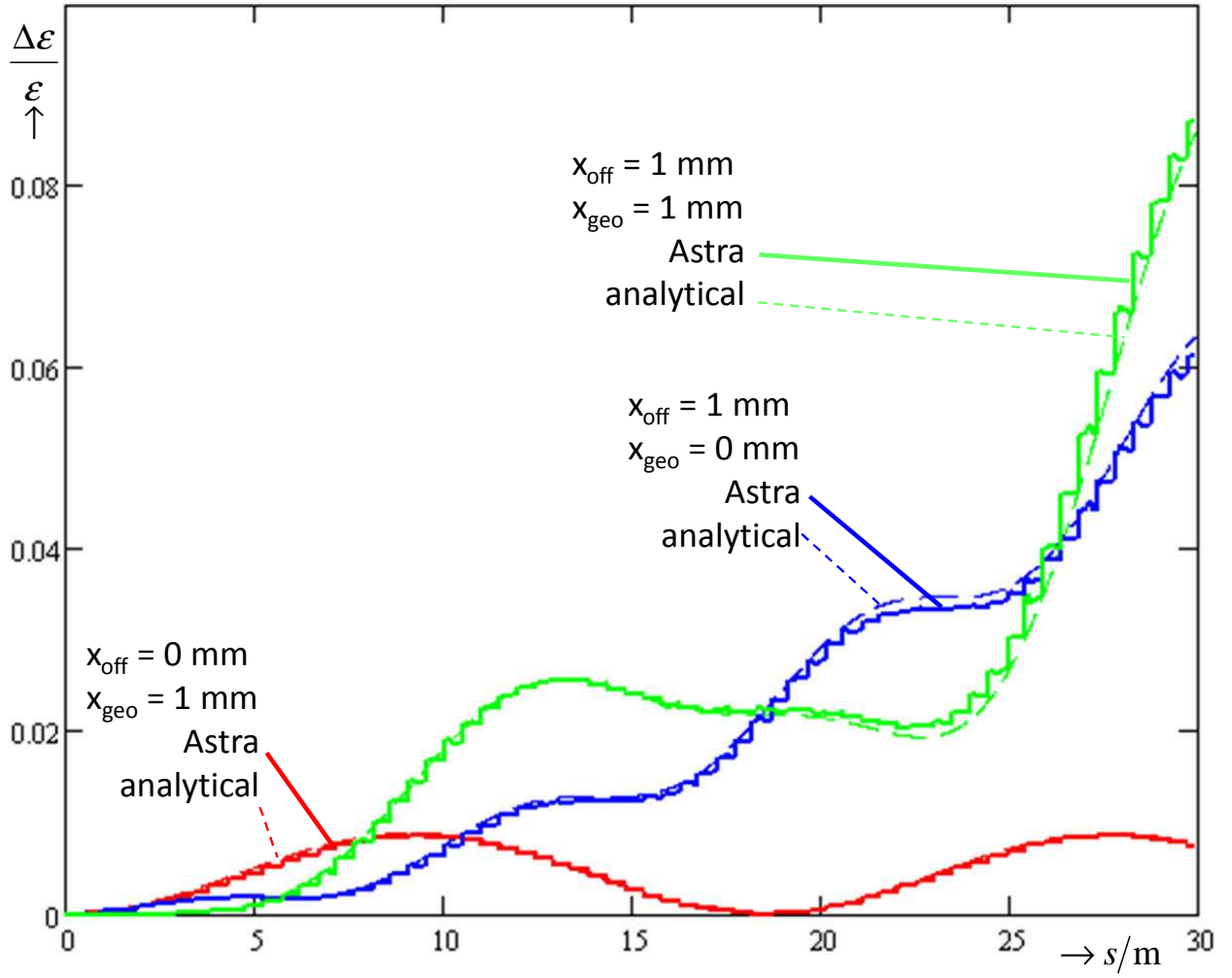


FIG. 4: Emittance growth along the undulator for dipole wakes in a stainless steel vacuum chamber with a radius of 4.75 mm: numerical simulation (solid line); analytical solution (dashed line).

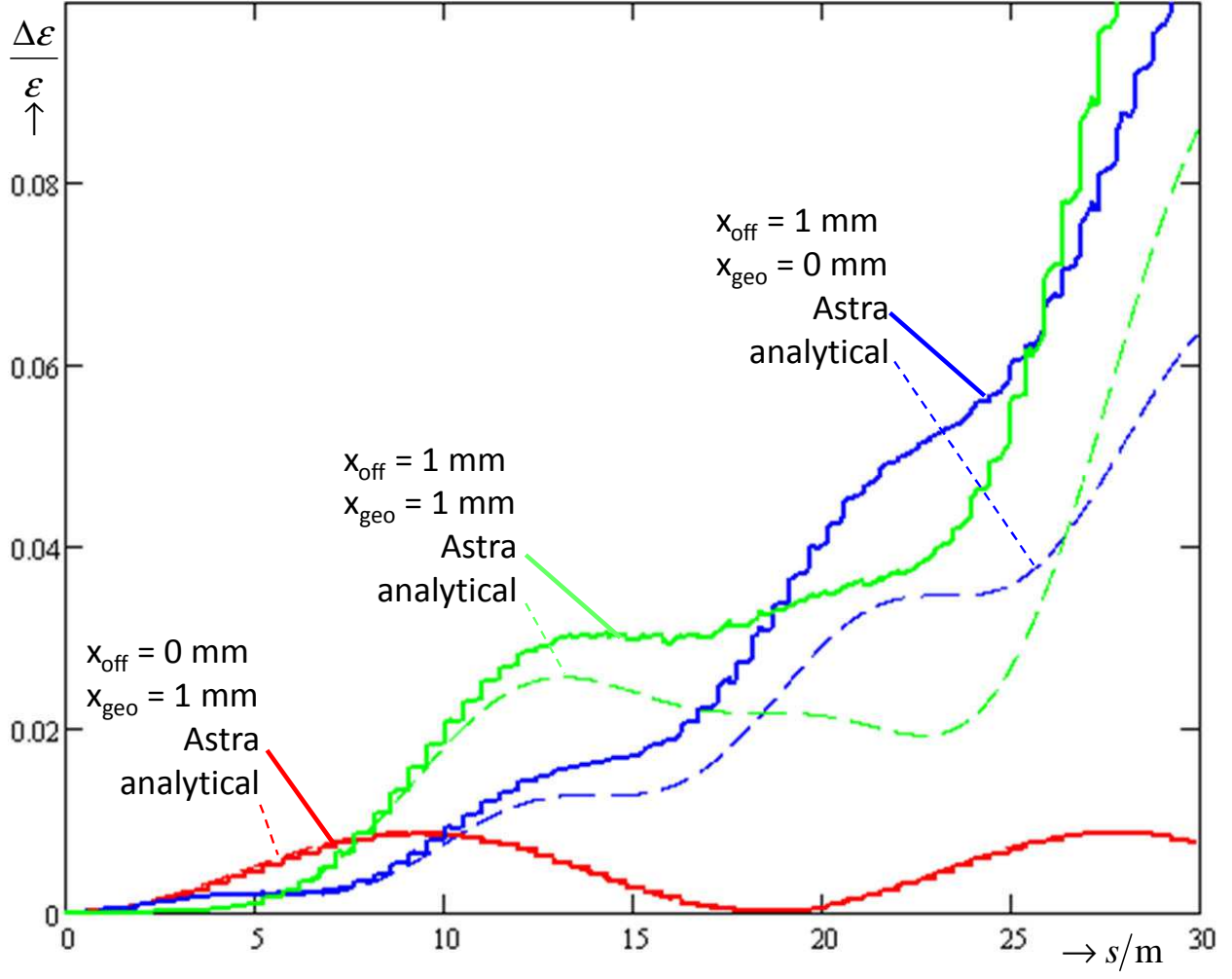


FIG. 5: Emittance growth along the undulator for monopole and dipole wakes in a stainless steel vacuum chamber with a radius of 4.75 mm: numerical simulation (solid line); analytical solution (dashed line).